ARTICLE - Non-Hodgkin Lymphoma

Low T-cell proportion in the tumor microenvironment is associated with immune escape and poor survival in diffuse large B-cell lymphoma

Joo Y. Song,[1] Mary Nwangwu,[2] Ting-Fang He,[2] Weiwei Zhang,[3] Hany Meawad,[1] Victoria Bedell,[1] Joyce Murata-Collins,[1] Pamela Skrabek,[4] Michel R. Nasr,[5] David Scott,[6] James Godfrey,[7] Peter Lee,[2] Wing C. Chan,[1] Dennis D. Weisenburger,[1,3] Anamarija M. Perry[8] and Alex F. Herrera[7]

[1]Department of Pathology, City of Hope Medical Center, Duarte, CA, USA; [2]Immuno-Oncology, Beckman Research Institute, City of Hope Medical Center, Duarte, CA, USA; [3]Department of Pathology and Microbiology, University of Nebraska Medical Center, Omaha, NE, USA; [4]Department of Hematology, CancerCare Manitoba, Manitoba, Canada; [5]Department of Pathology, SUNY Upstate Medical University, Syracuse, NY, USA; [6]British Columbia Research Center, Vancouver, British Columbia, Canada; [7]Department of Hematology & Hematopoietic Cell Transplantation, City of Hope Medical Center, Duarte, CA, USA and [8]Department of Pathology, University of Michigan, Ann Arbor, MI, USA

Correspondence: Joo Y. Song
josong@coh.org

Received: October 12, 2022.
Accepted: January 3, 2023.
Early view: January 12, 2023.

https://doi.org/10.3324/haematol.2022.282265

Supplemental Material

Methods

Cases with formalin-fixed, paraffin-embedded tissue (FFPET) were stained with hematoxylin and eosin (H&E) and re-reviewed to confirm the diagnosis of DLBCL, not otherwise specified (NOS). Immunohistochemistry (IHC) was performed on 3-4 micron sections of FFPET microarrays using antibodies to CD20, CD3, CD10, BCL6, MUM1, MYC, BCL2, B2M, HLA I, HLA II, and TIM3 (**Supplemental Table 2**). The slides were stained on an Ventana Discovery XT (Ventana, Tucson, AZ) for MYC, and on a Leica Bond III (Leica Biosystems, Chicago, IL) for all other stains and >30% positivity was considered positive. Of note, stains for B2M, HLA I, and HLA II showed membrane staining >70% of the tumor cells in the majority of positive cases and cases that were considered negative showed little or no staining of the tumor cells. TIM3 staining was reviewed and proportions were calculated using the QuPath v0.3.0 qualitative pathology and bioimage analysis software (https://qupath.github.io). Cases were reviewed and scored independently by three expert hematopathologists (JS, AP, MN). FISH cytogenetic analysis for *MYC*, *BCL2* and *BCL6* gene rearrangements was performed using the LSI dual color break-apart probes (Abbott Molecular, Des Plaines, IL). At least 100 nuclei were scored and rearrangement was defined as the presence of break-apart signals in ≥ 10% of the nuclei. Double/triple-hit lymphoma (DH) was defined as having concurrent rearrangements of *MYC* and *BCL2* and/or *BCL6* genes.

Mutation analysis

Tissue blocks in which >60% of the surface area consisted of tumor were selected for RNA and DNA extraction using the Qiagen Allprep RNA/DNA FFPET kit (Qiagen, Valencia, CA), following the manufacturer's recommended protocol. We used a custom targeted panel of 334 genes (designed by WCC), which includes the most frequently mutated genes in B-cell lymphoma, and performed DNA sequencing on an Illumina HiSeq 2500 (Illumina, San Diego, CA) as previously described (15).

Copy number analysis

The Oncoscan Copy Number Variation (CNV) assay (ThermoFisher, Waltham, MA) was performed according to the manufacturer's directions using 80 ng of DNA. The data files were analyzed with the Chromosome Analysis Suite (ThermoFisher). Briefly, the generation of these files entails calculating the log2 ratio, allelic difference and B-allele frequency (BAF), and then identifying normal diploid regions. Based on the normal diploid regions, the log2 ratio, allelic difference, and BAF are recomputed if necessary. Segmentation and visualization of the copy number abnormalities (CNAs) was performed with Nexus Copy Number™ 10.0 software (Bio Discovery, El Segundo, CA) using the SNP-FASST2 algorithm. The percent aberrant genome per case was calculated by taking the total size of the aberrant regions divided by the total size of the genome for chromosomes 1-22.

Gene expression analysis for classification

We used 200 ng of RNA on the nCounter platform (NanoString Technologies, Seattle, WA) to determine the cell of origin (COO) using the Lymphoma/Leukemia Molecular Profiling Project (LLMPP) code set Lymph2Cx (16). Briefly, the RNA was hybridized to custom code sets overnight at 65°C and processed on the nCounter Prep Station, and gene expression data was acquired on the nCounter Digital Analyzer. We then uploaded the data to the LLMPP website (https://llmpp.nih.gov) and generated the COO using the nSolver (NanoString Technologies, Seattle, WA). In addition, we also ran the DLBCL90 double-hit gene expression (DHIT) signature (17) on the nSolver. The DLBCL90 assay identifies the cell of origin and DH/TH with a *BCL2* translocation but was not designed to identify DH cases with a *BCL6* translocation. The DHIT signature (sig) scores were defined as DHITsig-positive (pos, greater than -6.3), DHITsig-negative (neg, less than -15.6), or DHITsig-indeterminate (ind, -6.3 to -15.6), as previously described(15, 17, 18).

Multispectral Immunofluorescence Tumor Analysis

Formalin-fixed, paraffin-embedded tissue (FFPET) specimens were cut at 3-4 µm sections and baked onto glass slides. The FFPET slides were then deparaffinized in 10-minute xylene washes (3x each), then rehydrated in decreasing ethanol concentration washes for 5 minutes (100%, 95%, 70%), with a final 5-minute wash in Milli-Q water. Heat-induced antigen retrieval was performed using AR9 buffer, 10x (pH 9) (AR9001KT, Akoya Biosciences, Marlborough, MA, USA) in a microwave oven for 20 minutes. A 2-minute Milli-Q water wash and a wash with TBS Automation Wash Buffer, 20X (TWB945M, Biocare Medical, Concord, CA, USA) were performed subsequently. Blocking was performed for 10 minutes using Antibody Diluent with Background-Reducing Components (S302283-2, Agilent, Santa Clara, CA, USA) to minimize non-specific background staining. Primary antibodies were incubated for 1 hour on a shaker at room temperature and was followed by a 10-minute incubation of horseradish peroxidase (HRP)-conjugated secondary antibody (Mach 2 Rabbit or Mouse HRP-Polymer) (RHRP520 L or MHRP520 L, Biocare Medical). Immunofluorescent labeling of antibodies was achieved using the Opal™ 7-color fluorescence IHC Kit (Akoya Biosciences) at a 1:100 dilution for 10 minutes. To perform multicolor immunofluorescent staining, the slides were serially stained with microwave incubation acting to remove previous antibodies while simultaneously exposing the next epitope of interest. After staining the final marker, cell nuclei were stained with DAPI (FP1490, Akoya Biosciences) and the slides were mounted with ProLong Gold Antifade Reagent (P36930, ThermoFisher Scientific, Waltham, MA, USA).

We utilized 2 multispectral immunofluorescence (mIF) panels: (1) CD3, CD4, CD8, PD-1, PAX5, DAPI; (2) CD163, CD79a, PAX5, PD-L1, CD56, DAPI. In the first panel, the primary antibodies used to serially detect the antigens of interest were CD3 (LN10, CD3-565-L-CE, Leica, Wetzler, Germany), CD8 (4B11, CD8-4B11-L-CE, Leica), PD-1 (NAT105, 315M-95, Cell Marque, Rocklin, CA, USA), CD4 (EP204, 104R-25, Cell

Marque), and Pax-5 (1EW, PA0552, Leica). The markers were visualized with Opal™ 520 TSA (FP1487001KT, Akoya Biosciences), Opal™ 540 TSA (FP1494001KT, Akoya Biosciences), Opal™ 650 TSA (FP1496001KT, Akoya Biosciences), Opal™ 570 TSA (FP1488001KT, Akoya Biosciences), and Opal™ 690 TSA (FP1497001KT, Akoya Biosciences) respectively.

In the second panel, the primary antibodies used to serially detect the antigens of interest were CD56 (123C3, M730429-2, Agilent), PD-L1 (SP142, ab228462, Abcam, Cambridge, UK), Pax-5 (1EW, PA0552, Leica), CD163 (10D6, CD163-L-CE, Leica), and CD79a (JCB117, M705029-2, Agilent). The markers were visualized with Opal™ 650 TSA, Opal™ 620 TSA (FP1495001KT, Akoya Biosciences), Opal™ 690 TSA, Opal™ 520 TSA, Opal™ 540 TSA, and Opal™ 570 TSA respectively.

Tissue slides were scanned using the Vectra 3.0 automated quantitative pathology imaging system (Akoya Biosciences) which initially captured fluorescent spectra of 10x resolution images in five channels (DAPI, FITC, Cy3, Texas Red, Cy5). Using a Phenochart™ whole slide viewer (Akoya Biosciences), regions of interest were established and chosen by the pathologist (JYS), and the selected images were acquired at 20x resolution in the same channels as the multispectral images (MSIs). After image capture, the MSIs were spectrally unmixed with inForm® tissue analysis software (Akoya Biosciences) and component TIFFs were exported. Proportion measures, nearest neighbor analysis, and spatial point pattern analysis were generated using Spotfire, and the resulting data output was visualized using GraphPad Prism.

Validation cohorts

Immune cellular proportion determination using gene expression profiling and CIBERSORTx

We used the gene expression profiling (GEP) data from 351 cases in the study of Lenz *et al* of *de novo* DLBCL (184 germinal center phenotype (GCB) DLBCL, 167 activated B-cell phenotype (ABC) DLBCL) treated with R-CHOP (19). We used the CIBERSORTx method (20) to determine the relative cell proportions (e.g. total T-cells, follicular helper T-cells, regulatory T-cells, NK-cells, and macrophages) in this independent cohort to confirm the relative cellular proportions by GEP.

Immunohistochemical staining for T-cells and digital scanning

To determine whether routine IHC would correlate with the findings by mIF, we used another independent cohort of 54 cases (University of Manitoba) of *de novo* DLBCL (37 GCB DLBCL, 17 ABC DLBCL) treated with R-CHOP. In addition, the 57 cases in the discovery cohort was stained by chromogenic IHC to evaluate the correlation of the IHC proportions to the proportions from the mIF. To ensure objective analysis of the stains and T cell proportions, cases on a TMA were stained with CD3, and PD1, scanned on the Ventana DP200 (Roche, Risch-Rotkreuz, Switzerland), and analyzed using the QuPath

v0.3.0 qualitative pathology and bioimage analysis software. From the digitally-imaged TMA stained for CD3 and PD1, the software determined the proportion of positive cells for each marker.

Statistical analysis

Logistic regression and survival analyses were performed using multiple parameters (nearest neighbor analysis, and T-cell subset, NK-cell, B-cell, and macrophage proportions). Cutoffs were determined using receiver operating characteristic (ROC) curves, and groups were categorized as high or low. The Mann-Whitney independent test and Fisher's exact test were used for continuous and non-continuous comparisons, respectively. Pearson's correlation coefficient (r) was determined. Medians with quartiles (1-4) were determined for continuous values. Overall survival (OS) and progression-free survival (PFS) were calculated, using the time from initial diagnosis to death due to any cause for OS. Patients alive at the last contact (OS) or patients alive without refractory/relapsed disease (PFS) were censored at the last contact. Survival was estimated using the Kaplan-Meier product-limit method (21). Hazard ratios (HR) and P values were determined using the Cox model. All P values were 2-sided and survival curves were generated using MedCalc Statistical Software version 19.1.5 (MedCalc Software bv, Ostend, Belgium).

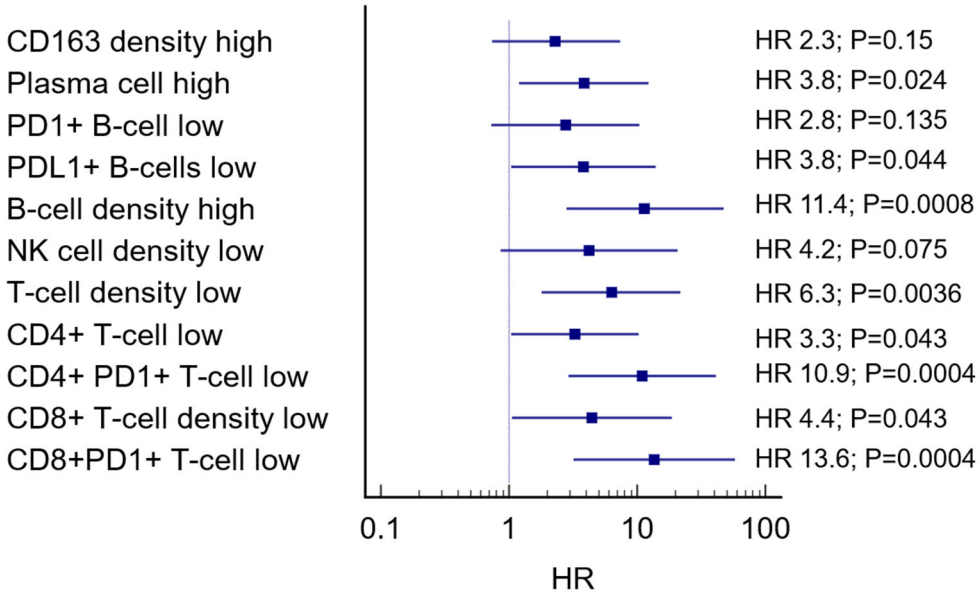

Supplemental Figure 1. Univariate analysis of cellular proportions with associated hazard ratios (HR).

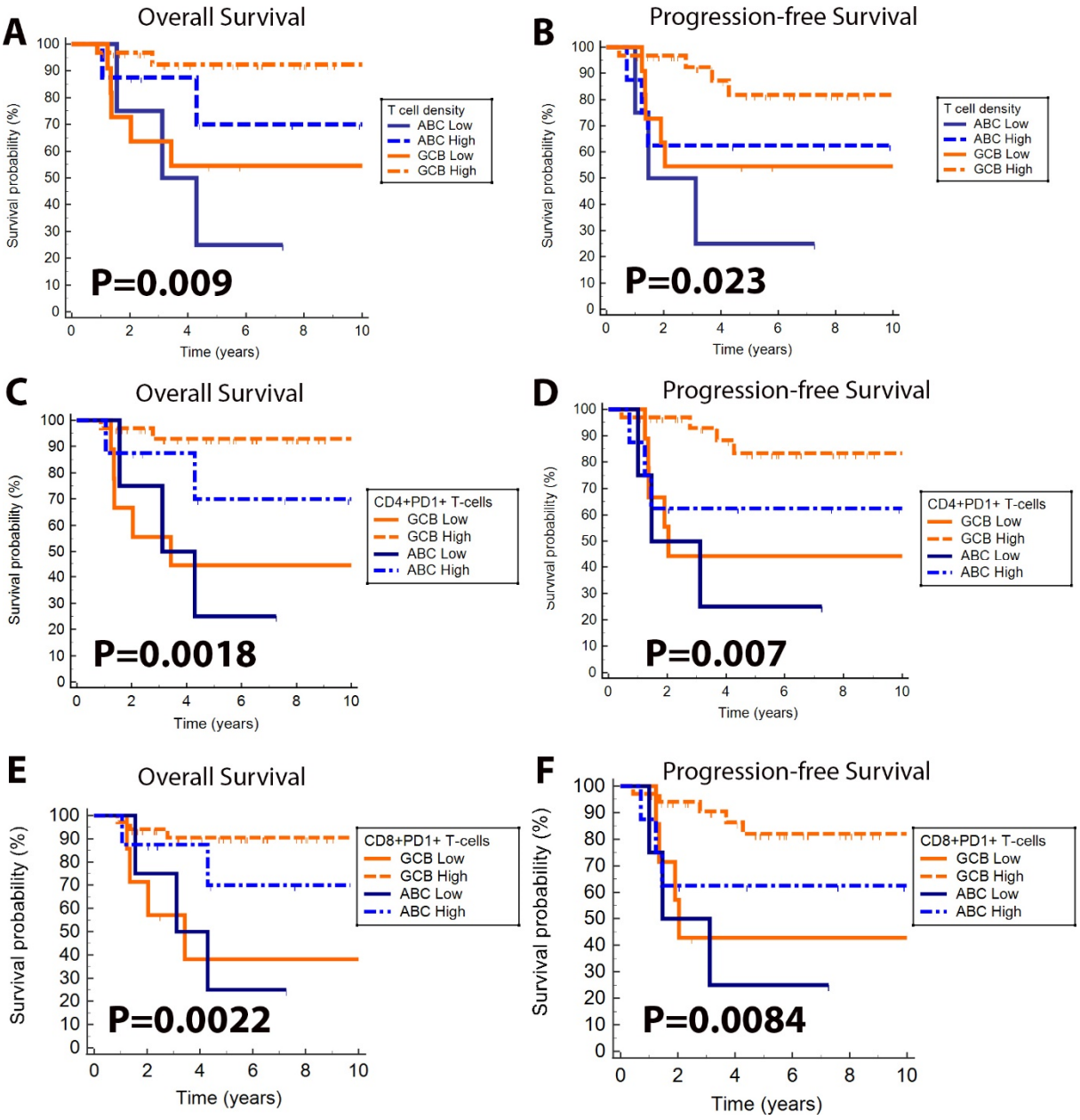

Supplemental Figure 2. Overall and progression-free survival based on cell-of-origin (COO) and overall T-cell proportion (A,B), CD4+PD1+ T-cells (C,D), and CD8+PD1+ T-cells (E,F).

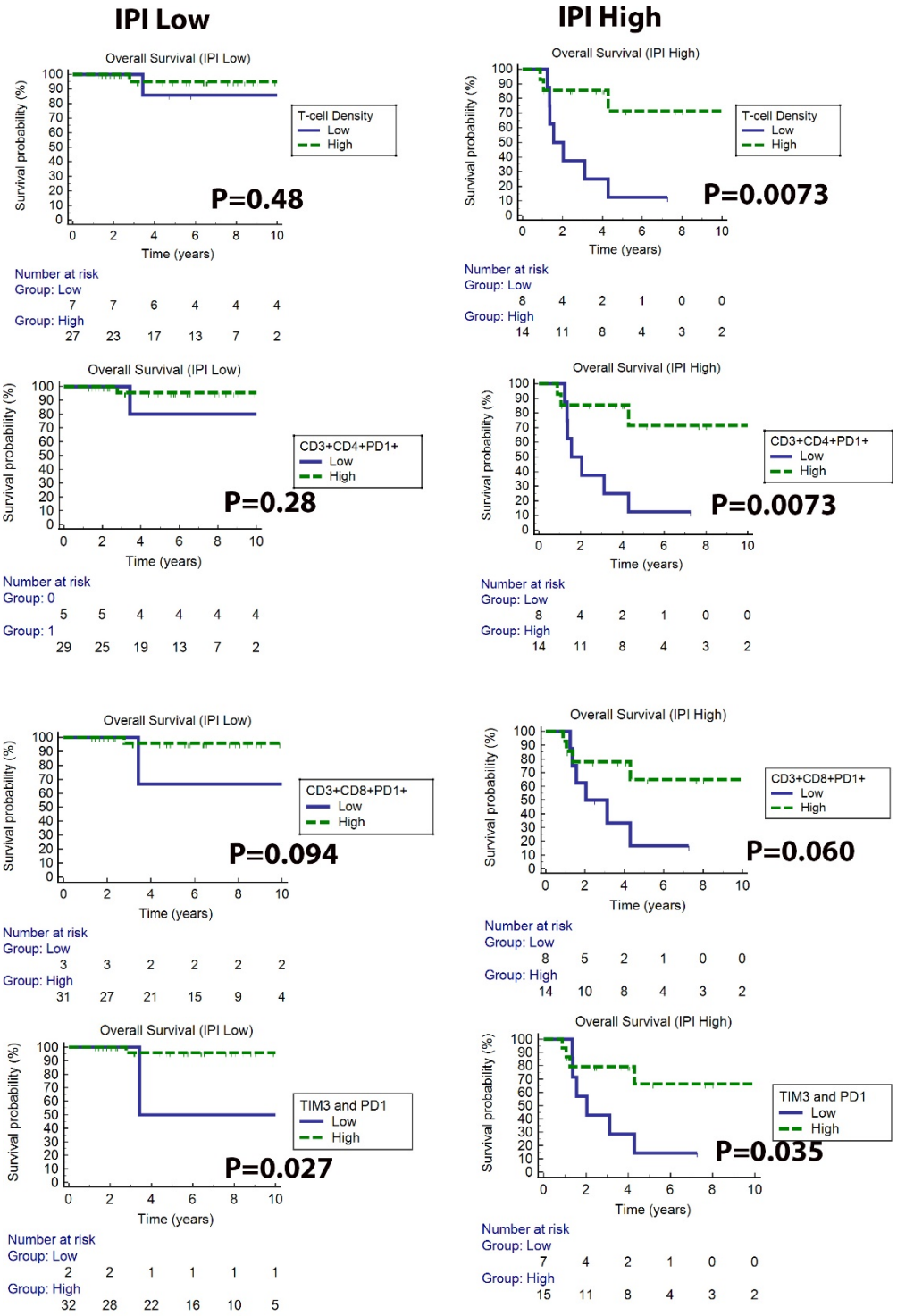

Supplemental Figure 3. Multivariate analysis adjusted for the IPI (Low=IPI 1,2; High=IPI 3,4) shows good OS with high T-cell proportion, high CD4+PD1+ T-cells, high CD8+PD1+ T-cells, and CD4+PD1+ T-cells with TIM3; particularly in the high IPI groups.

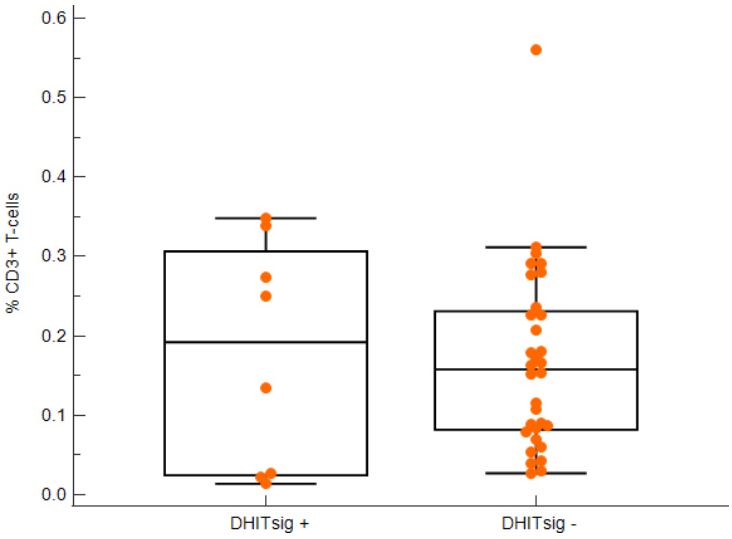

Supplemental Figure 4. Comparison of the T-cell proportion (Box-and-Whisker plot) in DHITsig-pos cases (median 19%, 95% CI: 2-34%) versus DHITsig-neg cases (median 16%, 95% CI: 9-21%) (P=0.95).

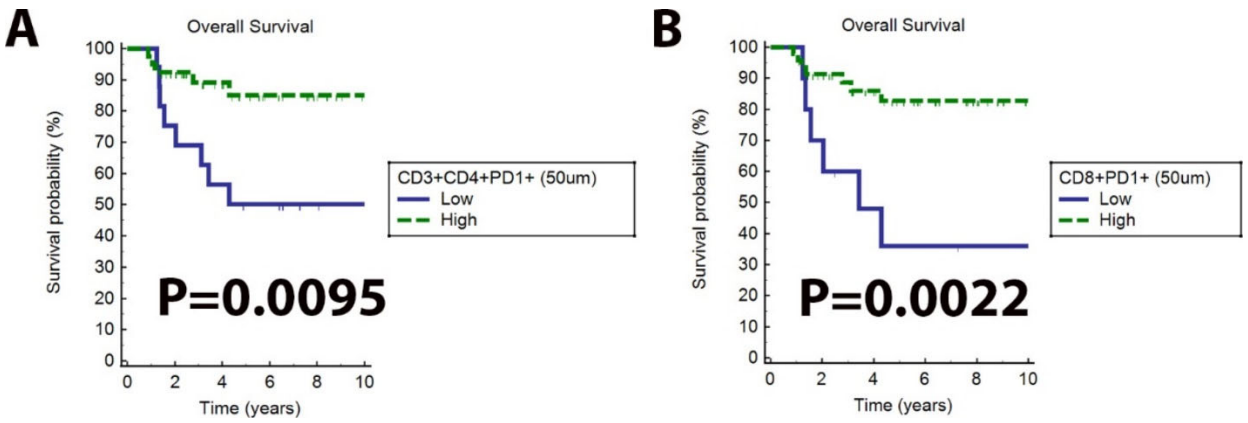

Supplemental Figure 5. Using nearest neighbor analysis, cases of DLBCL with higher numbers of CD4+PD1+ and CD8+PD1+ T-cells within close proximity (50 microns) to the tumor cells have better overall survival.

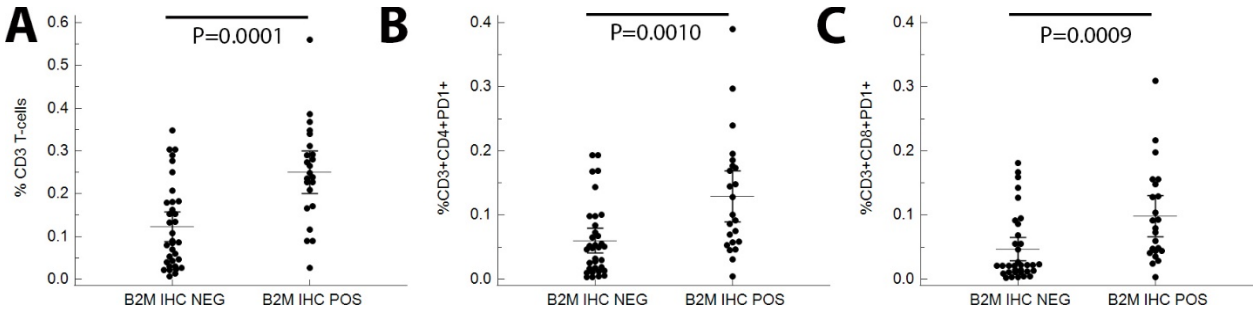

Supplemental Figure 6. T-cell proportions related to B2M immunohistochemistry (IHC) expression for (A) total T-cells, (B) CD3+CD4+PD1+ T-cells, and (C) CD3+CD8+PD1+ T-cells.

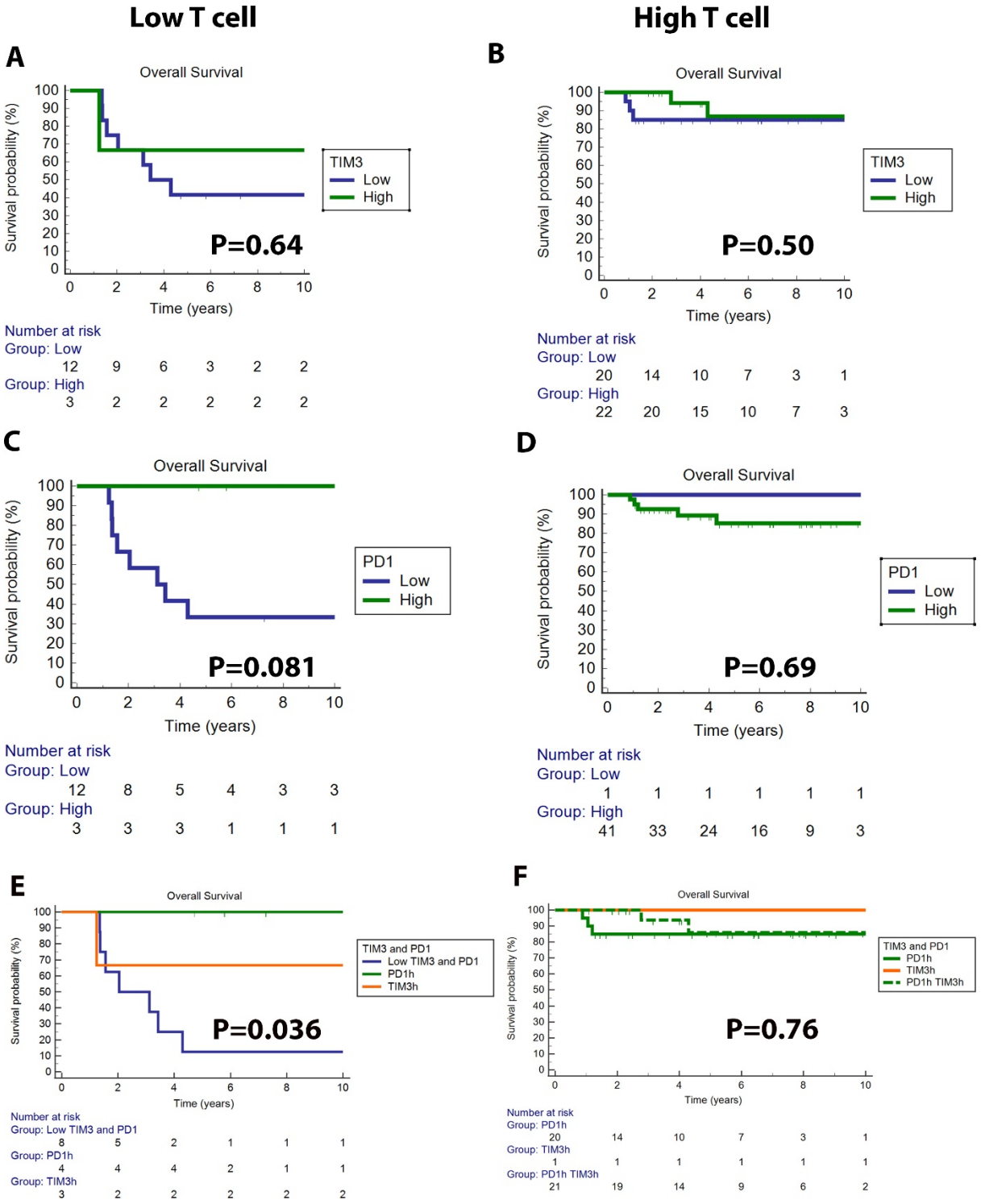

Supplemental Figure 7. TIM3 and PD1 expression within the low (left side) and high (right side) T-cell groups based on OS. The cases with low T cell content and low TIM3 and PD1 showed a poor OS (A, C, E). Cases with a high T-cell count showed most cases had a good prognosis (B, D, F). Of note, there was only one case with a low PD1

proportion (D) in the high T-cell group and there were no cases that had low PD1 and TIM3 (F).

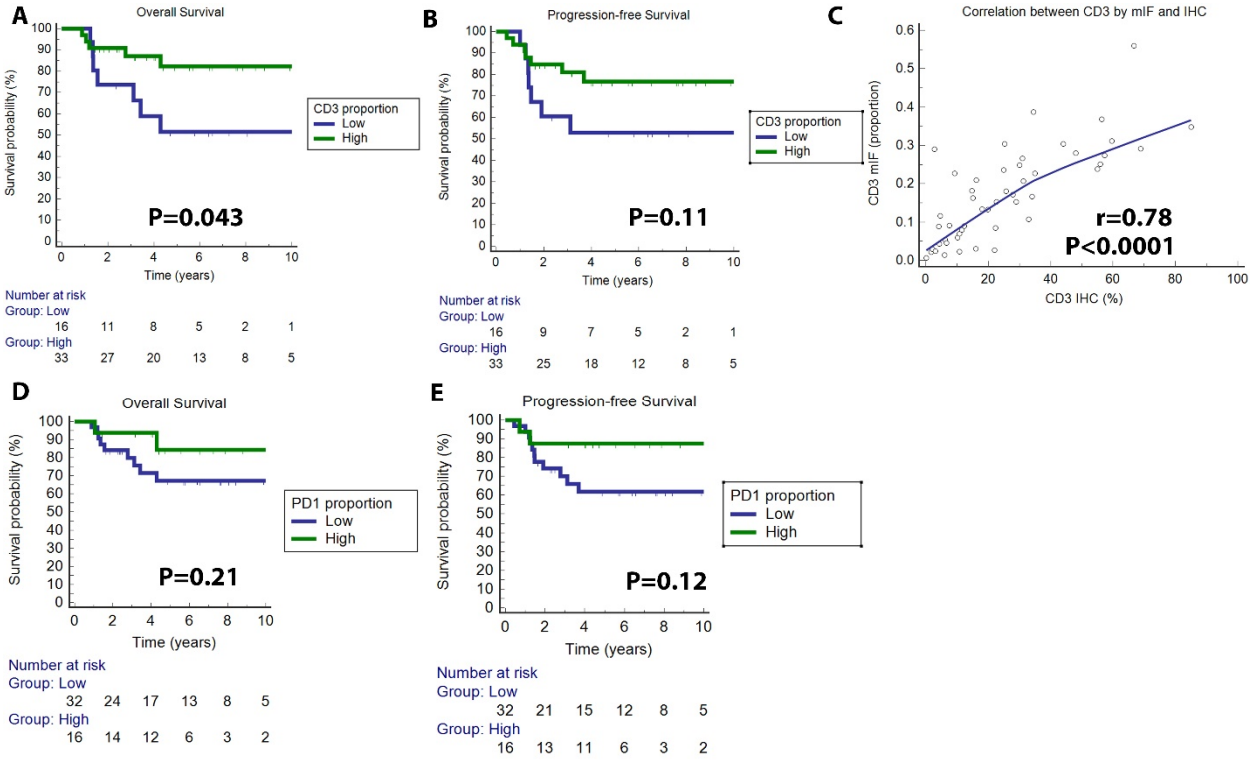

Supplemental Figure 8. Comparison of mIF by Vectra and chromogenic IHC in the discovery cohort of DLBCL (N=49 with CD3; N=48 with PD1). A. The overall survival (OS) with CD3 (ROC cutoff of 10.75%) shows significance while the B. progression-free survival (PFS) for CD3 shows a trend. C. There is good correlation between the mIF and IHC (r=0.78, P<0.0001, 95% CI 0.63-0.87). The PD1 IHC (ROC cutoff of 6.3%) cannot discriminate particular cell subsets but shows a trend with D. OS and E. PFS.

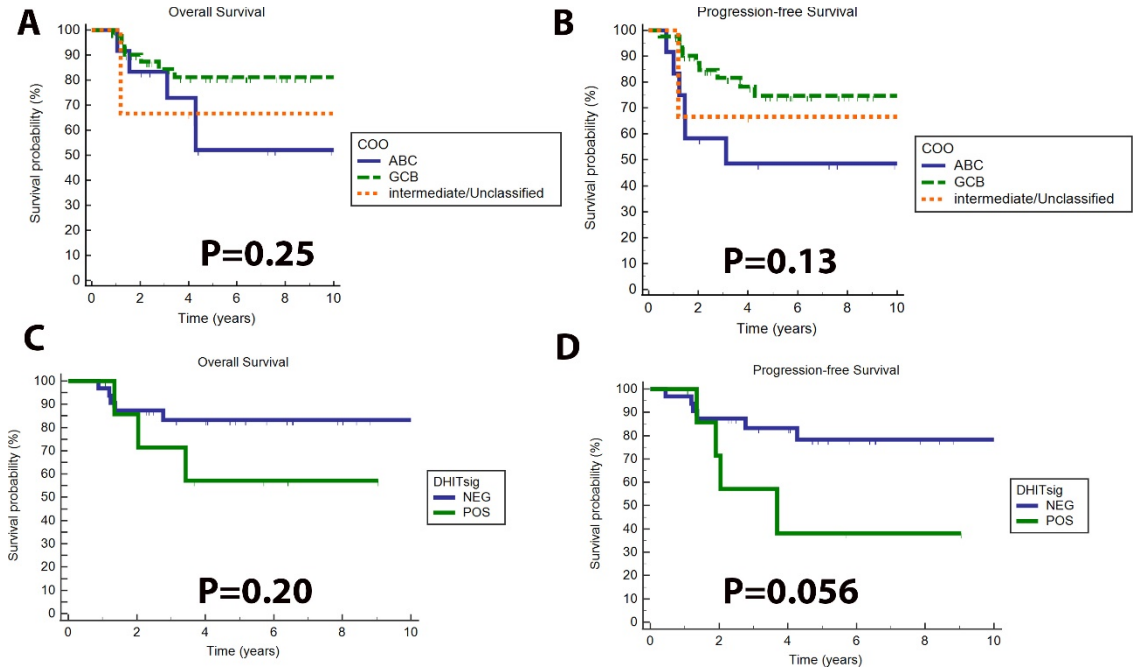

Supplemental Figure 9. A. Overall and B. progression-free survival of the DLBCL cohort based on cell-of-origin (COO). C. Overall and D. progression-free survival of the DLBCL cohort based on double-hit signature (DHIT) positive or negative.

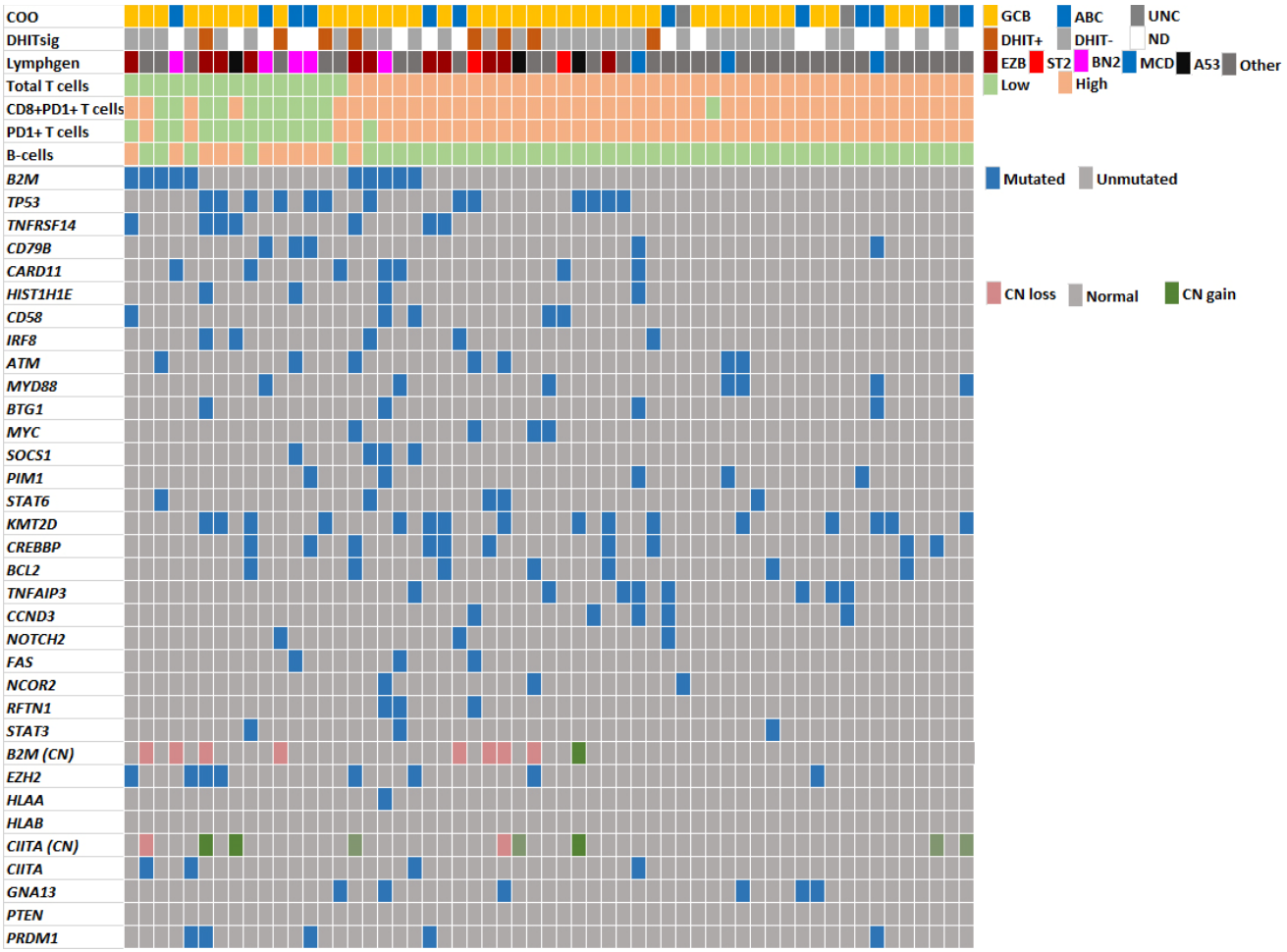

Supplemental Figure 10. Genomic profile of the 57 cases of de novo DLBCL with low and high T-cell content. Refer to legend in Figure 4.

Supplemental Table 1. Correlation of B2M, HLA I, and HLA II protein loss with T-cell proportion

IHC	Low T-cell proportion % (N)	High T-cell proportion %(N)	P value
B2M loss	93% (14/15)	48% (20/42)	P=0.002
HLA I loss	80% (12/15)	43% (18/42)	P=0.02
HLA II loss	93% (14/15)	57% (24/42)	P=0.01
Triple loss	73% (11/15)	26% (11/42)	P=0.002

IHC=immunohistochemistry, Triple loss=loss of B2M, HLA I, and HLA II.

Supplemental Table 2. Immunohistochemistry stains

Antibody	Clone	Company
CD3	2GV6	Ventana
CD20	L26	Ventana
CD10	SP67	Ventana
BCL2	SP66	Ventana
BCL6	GI191E/A8	Ventana
MUM1	MRQ-43	Ventana
c-MYC	Y69	Ventana
B2M	Poly	DAKO
HLA I	EMR8-5	Abcam
HLA II	CR3/43	DAKO
TIM3	D5D5R	Cell Signaling
PD1	Nat105	Ventana

Supplemental Table 3. Median T-cell proportions in relation to B2M, HLA I, and HLA II immunohistochemistry.

	B2M			HLA I			HLA II		
	+	-	P	+	-	P	+	-	P
CD3+ T-cell %	25% CI(21-29)	9% CI(5-16)	0.0001	24% CI(17-29)	9% CI(6-17)	0.0013	23% CI(10-27)	14% CI(7-20)	0.14
CD3+CD4+PD1+ %	10% CI(6-17)	5% CI(2-7%)	0.0010	10% CI(6-17)	5% CI(3-7)	0.0040	9% CI(5-17)	5% CI(3-8)	0.041
CD3+CD8+PD1+ %	8% CI(1-5)	2% CI(5-13)	0.0009	8% CI(5-13)	2% CI(1-4)	0.0011	6% CI(2-11)	3% CI(2-6)	0.15

+=positive, -=negative, CI=95% confidence interval, P=P value